

Report

**R-20-03**

September 2021



# Monitoring bentonite porewater chemistry using electrochemical sensors

**Taylor Martino**  
**Mengnan Guo**  
**James J Noël**

SVENSK KÄRNBRÄNSLEHANTERING AB

SWEDISH NUCLEAR FUEL  
AND WASTE MANAGEMENT CO

Box 3091, SE-169 03 Solna  
Phone +46 8 459 84 00  
skb.se

SVENSK KÄRNBRÄNSLEHANTERING



ISSN 1402-3091

**SKB R-20-03**

ID 1880608

September 2021

# Monitoring bentonite porewater chemistry using electrochemical sensors

Taylor Martino, Mengnan Guo, James J Noël  
Western University, London, Ontario

*Keywords:* Bentonite, Clay, Copper, Chloride, pH, Waste container, Porewater, Electrochemical sensors, Corrosion, Groundwater, Deep geologic repository.

This report concerns a study which was conducted for Svensk Kärnbränslehantering AB (SKB). The conclusions and viewpoints presented in the report are those of the authors. SKB may draw modified conclusions, based on additional literature sources and/or expert opinions.

This report is published on [www.skb.se](http://www.skb.se)

© 2021 Svensk Kärnbränslehantering AB



# Abstract

The Scandinavian plan for the permanent disposal of spent nuclear fuel features a multi-barrier system design which includes the fuel itself, a specially designed copper waste container, bentonite clay buffer and the deep geologic repository (DGR). This report focuses on the chemistry of the bentonite clay buffer material. Bentonite is an ideal buffer material due its ability to swell upon contact with groundwater, which provides a seal around the container upon repository saturation. The swelling feature of the clay is a consequence of the large amount of montmorillonite present in the bentonite. It has a 2:1 silica and alumina sheet structure, which separates upon intercalation of groundwater, thus causing swelling. As the groundwater saturates the clay, its chemical composition may be altered due to interactions with minerals present in the clay, thus the aqueous phase that comes into contact with the container after passing through the clay may be different than the repository groundwater. It is important to determine the composition of this aqueous phase in order to better understand the container environment in the DGR.

In this study electrochemical sensors were employed to monitor bentonite water chemistry over time under saline and oxic conditions. A new experimental set-up was developed in which a bentonite clay disk was exposed to solution and changes in pH, chloride concentration and corrosion potential of copper in the clay and on its opposite surface were monitored. Sensors were positioned on the disk surface and embedded in the clay to determine any differences between surface water (that has passed through the bentonite) and free porewater inside the compacted bentonite disk. While it remains uncertain whether or not the different types of water can be identified, this study yields insight into chemical properties of the bentonite clay upon exposure to saline solutions.



# Contents

<b>1</b>	<b>Introduction</b>	7
<b>2</b>	<b>Experimental</b>	9
2.1	Solution preparation	9
2.2	Electrode preparation	9
2.2.1	Reference electrodes	9
2.2.2	pH electrodes	10
2.2.3	Ion specific electrodes	10
2.2.4	Cu electrodes	10
2.3	Bentonite disk preparation	11
2.4	Set-up and instrumentation	12
<b>3</b>	<b>Results</b>	13
3.1	Electrode stability and calibrations	13
3.1.1	Embedded reference electrode stability	13
3.1.2	pH electrode calibration	14
3.1.3	Ion specific electrode calibration	14
3.2	Initial bentonite porewater measurements	15
3.3	Testing the validity of the experimental set-up	18
3.3.1	Stability of the agar reference electrode	18
3.3.2	Measuring membrane potentials across the bentonite clay disk	20
<b>4</b>	<b>Key results and future work</b>	27
	<b>References</b>	29



# 1 Introduction

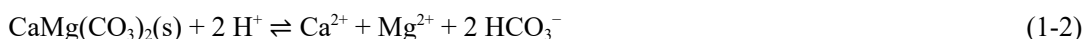
Nuclear energy is a reliable, inexpensive, and environmentally friendly source of electrical power. However, with the production of spent nuclear fuel, development of a safe containment and storage program must be implemented. One approach proposed in many countries, including Sweden, Finland and Canada, is permanent disposal of the spent fuel in a deep geological repository (DGR). For the Scandinavian plan, the spent fuel is to be placed in specially designed containers fabricated with a cast iron inner vessel and an outer copper shell; these materials are designed to avoid both corrosion and mechanical failure. The outer shell would be fabricated using P-deoxidized Cu with a thickness of 50 mm (King et al. 2010, 2013 King 2002). It is proposed that these containers be buried in crystalline rock approximately 500 m below the surface and that the excavated boreholes be backfilled with bentonite clay (Berglund and Lindborg 2017).

Bentonite is an ideal buffer material due to its swelling and buffering capabilities. It is composed of > 75 % montmorillonite, which has a structure of 2:1 silica and alumina sheets, and accessory minerals (minerals present in small quantities) including gypsum ( $\text{CaSO}_4 \cdot \text{H}_2\text{O}$ ), halite ( $\text{NaCl}$ ), pyrite ( $\text{FeS}_2$ ) and calcite ( $\text{CaCO}_3$ ) (Cuevas et al. 1997). The sheet-type structure allows for swelling upon contact with groundwater, as it is strongly hygroscopic. Due to spatial constraints of the boreholes, the swollen clay acts as a self-sealing medium, sealing itself around the buried container and filling any openings in the repository. It is a porous material with a low hydraulic conductivity ( $< 10^{-12}$  m/s) which limits mass transport processes entirely to diffusion, with diffusion being two orders of magnitude slower in bentonite than in bulk solution. Low conductivity in conjunction with strong water adsorption allows the highly compacted clay to act as an effective barrier against degradation processes. It limits mass transport of species to and from the container surface, prevents microbial activity close to the container surface and possesses the ability to capture cationic species (and therefore a large proportion of radionuclides) by ion exchange processes (King 2009, 2013). Due to the presence of the bentonite buffer, the composition of the aqueous phase in contact with the container surface may significantly differ from that of groundwater, at least for a significant time period; thus determination of the composition of this phase is crucial as it must be compatible with the container material.

Several theories have been used to describe the bentonite porewater, or aqueous phase mentioned previously, and it is generally characterized into three main types: (i) free porewater consisting of a charge-balanced aqueous solution of anions and cations; (ii) interlayer water containing water and cations between montmorillonite layers which is devoid of anions and thus in a charge deficit; (iii) electrostatic double layer (between mineral surface and free water) containing water, cations and a small concentration of anions, with the excess cation charge balanced by the negatively charged outer surface layer of the montmorillonite (Bradbury and Baeyens 2003). The quantity of each type of water present is not constant within the clay; it varies as a function of dry density, salinity of the solution and/or the amount of accessory minerals present (Idiart and Pękala 2016). Many models have been used to correctly predict the chemistry of the various types of bentonite porewater, including the Donnan equilibrium, Poisson-Boltzmann, and multi-porosity models. Correct modeling of the bentonite porewater is necessary in understanding how the aqueous phase in contact with the Cu container will evolve over long periods of time.

There are three main reactive sites on the bentonite that have the ability to alter porewater chemistry, (i) the electric double layer where electrostatically bound cations can exchange with solution, (ii) the montmorillonite sheets that carry a permanent negative charge due to substitution of lattice cations which carry charges always less than the sum of the charges of the anionic centres on a sheet and (iii) amphoteric surface hydroxide groups that can become protonated and deprotonated as the pH changes (Bradbury and Baeyens 2009).

The pH of the bentonite porewater is found to be around 8; this is likely governed by the dissolution of carbonate-containing minerals such as calcite ( $\text{CaCO}_3$ ), dolomite ( $\text{CaMg}(\text{CO}_3)_2$ ) and siderite ( $\text{FeCO}_3$ ) (Bruno et al. 1999, Arcos et al. 2006).



Another important porewater constituent that affects bentonite porewater chemistry is the chloride anion. At the Olkiluoto site in Finland, infiltrating groundwater contained chloride concentrations ranging from 0.03 M to 0.45 M and it was estimated that the chloride concentration of the groundwater present in the DGR after 100 000 years of container emplacement would decrease to  $\sim 0.01$  M (King et al. 2010). The predicted decrease in chloride concentration over time can be attributed to the infiltration of dilute waters as a result of glacial cycles (Auqué et al. 2006).

Various studies of the corrosion of Cu in bentonite have been conducted under oxic and saline groundwater conditions. Rosborg and Pan (2008) monitored the corrosion of Cu exposed to a bentonite test parcel in Äspö Hard Rock Laboratory. The study concluded, using electrochemical impedance spectroscopy (EIS), that the corrosion resistance of Cu was primarily dependant on the formation of a thin, passive cuprite ( $\text{Cu}_2\text{O}$ ) film that initially formed over 3 days, and a porous outer layer of  $\text{Cu}_2\text{O}$  that formed slowly and was detected by EIS after 5 months of exposure. It was found that the outer porous layer partially intermixed with the bentonite clay. Rosborg et al. (2011) and Kosec et al. (2015) used electrical resistance (ER) sensors and EIS to monitor Cu corrosion over three-year and four-year exposure periods. ER sensors and EIS measurements revealed a corrosion rate of 1 to  $0.4 \mu\text{m/a}$ . This extensive study concluded that corrosion occurred via non-uniform growth governed by diffusion of Cu species into the surrounding bentonite. X-ray diffraction (XRD) and Raman spectroscopy determined that the corrosion product was composed of  $\text{Cu}_2\text{O}$  and paratacamite ( $\text{Cu}_2(\text{OH})_3\text{Cl}$ ). While the corrosion rates were evaluated in these studies, the effect of solution chemistry was not discussed.

The purpose of this study was to develop an experimental set-up in which electrochemical sensors could be employed to monitor the pH, chloride concentration, and corrosion potential ( $E_{\text{corr}}$ ) of Cu in bentonite porewater under oxic conditions. Surface and embedded electrode measurements were made to observe any discrepancy between the surface and embedded sites. Distinguishing the chemistry between the sites will provide important information with respect to future model validation and determination of the composition of the aqueous phase that will ultimately be in contact with the canister in the DGR.

## 2 Experimental

### 2.1 Solution preparation

Electrolytes were prepared with Type-1 water obtained from a Thermo Scientific Barnstead Nanopure 7143 water system. Solutions were made from reagent-grade NaCl, 99.0 % assay (Caledon Laboratory Chemicals) and H<sub>2</sub>SO<sub>4</sub>, 95 % to 98 % assay (Caledon Laboratory Chemicals). NaCl solutions between 0.1 M and 1.0 M were prepared for electrode fabrication and calibration as well as for bentonite experiments. A 0.5 M H<sub>2</sub>SO<sub>4</sub> solution was prepared for electrode fabrication.

### 2.2 Electrode preparation

#### 2.2.1 Reference electrodes

A micro-Ag/AgCl (3.0 M) reference electrode (Microelectrodes, Inc.) was used for the bentonite surface measurements presented in Section 3.2. A Pd-H reference electrode was fabricated with Pd wire (0.5 mm diameter, Alfa Aesar) and cathodically charged in 0.5 M H<sub>2</sub>SO<sub>4</sub> at  $-5.0 \times 10^{-3}$  A for a range of durations from 2 h up to 20 h. A graphene oxide (GO) Ag/AgCl reference electrode was fabricated based on a previously published procedure (Kim et al. 2015). A Ag/AgCl electrode was prepared by applying a  $2.0 \times 10^{-3}$  A current to a Ag wire (1.2 mm diameter) in 1 M NaCl for 20 min. A suspension of GO with a concentration of 1.375 g/L was prepared from dry GO flakes (Graphene Supermarket) and Type-1 water, and drop-casted onto the Ag/AgCl wire, which was then dried on a hot plate at 40 °C.

A new Ag/AgCl/KCl agar/polychloroprene reference electrode was fabricated, based on a paper by Liao and Chou (2006). An Ag/AgCl electrode was prepared via the procedure described previously. The KCl agar was prepared using agar powder (Alfa Aesar) and saturated KCl solution (1 g agar dissolved in 25 mL of KCl solution) and used to coat the Ag/AgCl wire. Polychloroprene (Sigma Aldrich) was degraded in CH<sub>2</sub>Cl<sub>2</sub> (Caledon Laboratory Chemicals) via heating and stirring until it approximately doubled in size, and was then wrapped around the Ag/AgCl/KCl agar wire, as shown in Figure 2-1. This electrode, however, was quite difficult to fabricate. In a second design of the Ag/AgCl/KCl agar/polychloroprene electrode, shrink tubing of two differing diameters was used to construct the body of the electrode: 2.36 mm fluorinated ethylene propylene (FEP) (Zeus) and 3.05 mm polytetrafluoroethylene (PTFE) (Zeus). A schematic of the electrode is shown in Figure 2-2a. The 3.05 mm tubing was cut to the length of the Ag/AgCl electrode, leaving room to make an electrical connection, and  $\frac{1}{4}$  of this tubing was shrunk to a thickness similar to that of the Ag wire. A small portion of the 2.36 mm tubing was shrunk onto the Ag wire to ensure the PTFE tubing fit properly onto the Ag/AgCl electrode. The prepared agar was then injected into the tubing using a syringe and the degraded polychloroprene was stretched over the small opening. The addition of the shrink tubing eliminated fabrication difficulties associated with the initial design. The re-designed electrode was used for all agar reference electrode measurements presented in this report.

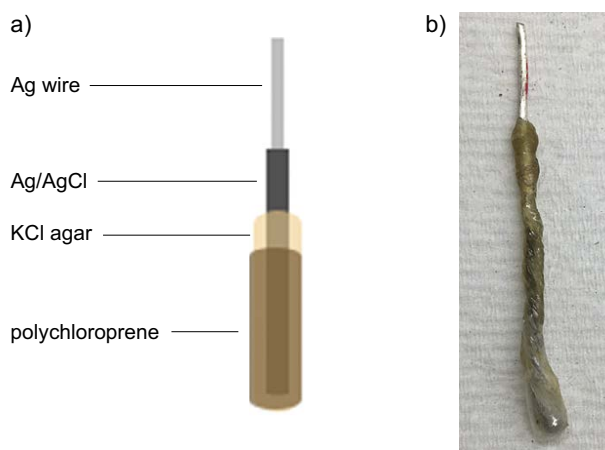


**Figure 2-1.** Schematic (a) and photograph (b) of the initial Ag/AgCl/KCl agar/polychloroprene reference electrode.

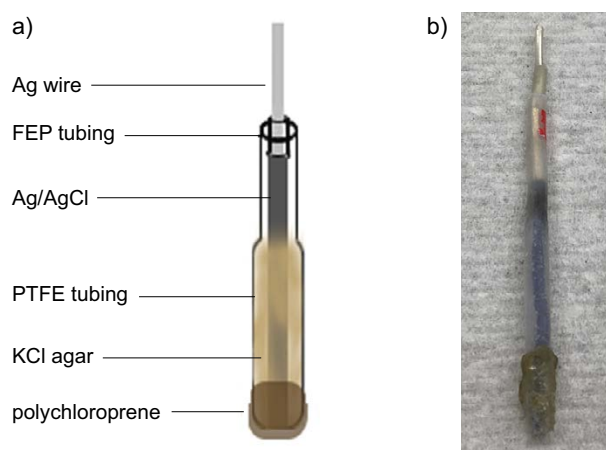


**Figure 2-2.** Schematic (a) and photograph (b) of the newly designed Ag/AgCl/KCl agar/polychloroprene reference electrode.

### 2.2.2 pH electrodes

The embedded iridium oxide electrode was fabricated using an iridium wire (0.25 mm diameter) that was ground using SiC paper (grit size: 1200). The iridium oxide film was grown, based on a method by Hitchman and Ramanathan (1988), via cyclic voltammetry in 0.5 M H<sub>2</sub>SO<sub>4</sub> (Caledon Laboratory Chemicals), scanning from -0.25 V/SCE to 1.25 V/SCE for 4 hours at a scan rate of 3 V/s. Based on the results of stability tests we conducted, the electrode was then left to stabilize in air for a minimum of 4 days. The latter step deviates from the procedure of Hitchman and Ramanathan, who scanned their electrode slowly prior to pH measurements. This was not feasible in our experiments, as the electrode would be in continuous use for periods of weeks, so we stabilized the electrode first to minimize changes during the operational period.

The surface iridium oxide electrode was made using an Ir wire (0.5 mm diameter, Alfa Aesar) set in a glass tube using epoxy resin. The cross-section was ground using SiC papers (grit sizes: 800, 1000, 1200, and 2400) prior to film growth. The electrode was subsequently immersed in Type-1 water overnight and then left to stabilize in air for a minimum of 4 days. Electrodes were calibrated in buffer solutions of pH 4, 7 and 10 (Caledon Laboratory Chemicals).

### 2.2.3 Ion specific electrodes

The embedded electrode was fabricated using a Ag wire (1.2 mm diameter) that was ground using SiC papers (grit sizes: 1200 and 2400). The AgCl film was grown by applying an anodic current of 10<sup>-3</sup> A in 1.0 M NaCl solution for 20 min. For the surface electrode, a Ag wire (1.2 mm diameter) was set in a glass tube using epoxy resin. The cross section was ground using SiC papers (grit sizes: 800, 1000, 1200, and 2400) prior to film growth. The AgCl film was grown by applying an anodic current of 5 × 10<sup>-5</sup> A for 20 min in 1.0 M NaCl. Each electrode was calibrated using NaCl solutions ranging in concentration from 0.01 M to 1 M.

### 2.2.4 Cu electrodes

Cu electrodes were fabricated for both embedded and surface measurements. The embedded electrode was a Cu wire (1.75 mm diameter, Belden), ground using SiC papers (grit sizes: 800, 1000, 1200, and 2400). The surface electrode was composed of a Cu wire (1.65 mm diameter, A = 2.14 mm<sup>2</sup>) set in a glass tube with epoxy resin. The cross-section was ground using SiC papers (grit sizes: 800, 1000, 1200, and 2400), and subsequently polished to a mirror finish using Al<sub>2</sub>O<sub>3</sub> suspensions (1 μm, 0.3 μm, and 0.05 μm).

### 2.3 Bentonite disk preparation

MX-80 bentonite, pre-moistened to 16.7 % moisture (calculated as mass of water / (mass of water + mass bentonite)  $\times$  100), was pressed into disks with a dry density of 1.6 g/cm<sup>3</sup> and a radius of 2 cm with varying thickness. The disks were compacted using specially designed mold and dies, shown in Figure 2-3. The electrodes to be embedded were placed into the base of the press and covered with the bentonite clay. The press was then assembled, and bentonite compacted using an arbor press. The mold was disassembled and the bentonite disk with the embedded electrodes was then removed and transferred to the specially designed holder (discussed in Section 2.4).

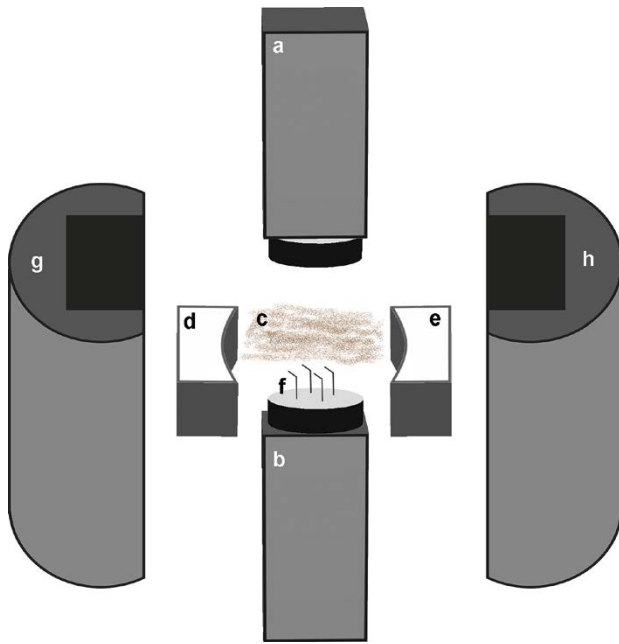


**Figure 2-3.** Schematic of the disassembled bentonite mold and dies: (a/b) dies; (c) bentonite clay; (d/e) Teflon insert; (f) embedded electrodes; (g/h) outer mold.

## 2.4 Set-up and instrumentation

A two-piece polytetrafluoroethylene (PTFE) holder, shown in Figure 2-4, was designed to ensure surface/embedded electrode contact with the bentonite clay disk during the experiment. The top of the holder had holes for each electrode, shown in Figure 2-4a; this allowed for electrical connections to be made while the electrodes were in contact with the bentonite disk. The bottom of the holder, shown in Figure 2-4b, held the clay disk and had a series of tiny holes that allowed for exposure of the bentonite to solution. The inside of the bottom component was covered with filter paper to ensure that no bentonite was lost through the holes. The holder with the bentonite and electrodes was held over the solution using a retort stand. The open circuit potential ( $E_{oc}$ ) and corrosion potential ( $E_{corr}$ ) measurements were collected using an IOTech ADC488/16A analog-to-digital converter and monitored using ADC488 control software.

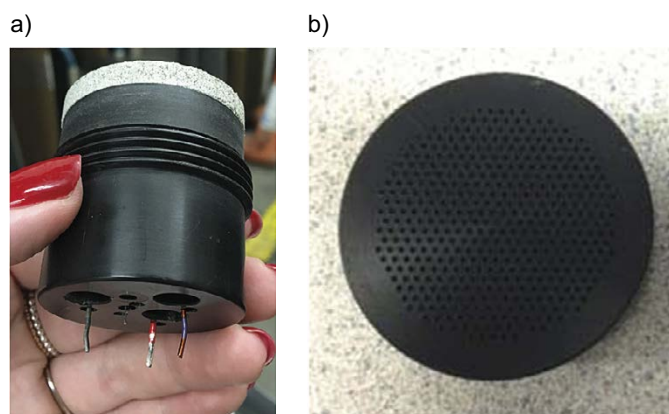


**Figure 2-4.** Two-piece bentonite holder; (a) top piece with clay and embedded electrodes and (b) bottom portion with a grid of tiny holes to allow for solution ingress.

## 3 Results

### 3.1 Electrode stability and calibrations

#### 3.1.1 Embedded reference electrode stability

The reference electrode selected for embedded measurements must be stable for the duration of the experiment, insensitive to changes in pH and  $[\text{Cl}^-]$ , and able to withstand the pressure of the embedding process. The pressure associated with the bentonite disk compaction makes it impossible to use traditional glass-body reference electrodes. The first embedded reference electrode tested was a Pd-H electrode. The electrode, however, proved not to be stable for the duration of the experiment, irrespective of how long it was charged, and it was also sensitive to pH changes. The next electrode tested was the Ag/AgCl/GO electrode, where the GO coating provided an interlocked and layered structure known to exhibit good mechanical strength (Kim et al. 2015). The electrode was found to be stable and insensitive to changes in pH; however, like a traditional Ag/AgCl electrode, it was  $\text{Cl}^-$  sensitive. The electrode was fabricated many times with emphasis on thickening of the GO outer layer in order to prevent  $\text{Cl}^-$  from reaching the AgCl film, but the electrode remained  $\text{Cl}^-$ -sensitive.

Many solid-state reference electrodes have been fabricated based on a Ag/AgCl electrode with a layer-by-layer assembly of various immobile electrolytes and polymers, often including Nafion (Kinlen et al. 1994, Kwon et al. 2007, Nolan et al. 1997). However, synthesis of these electrodes can be complex, and Nafion is expensive; thus such electrodes are not practical as embedded sensors because a new electrode would have to be fabricated for each experiment, as the electrode cannot be removed non-destructively from the bentonite after measurements have been completed. Huang et al. (2003) proposed covering a Ag/AgCl electrode with agar gel made with saturated KCl solution. The KCl agar would provide a saturated  $\text{Cl}^-$  environment around the Ag/AgCl electrode, thus allowing it to maintain a stable potential over time and be  $\text{Cl}^-$ -insensitive. The electrode proved to be stable, as well as insensitive to changes in either pH or  $[\text{Cl}^-]$ , however the gel dissolved and fell off the electrode after 60 h; it would also have been unable to withstand the embedding process. Liao and Chou (2006) proposed a planar Ag/AgCl/KCl agar electrode in which the agar was coated with chloroprene as a protective layer. A wire Ag/AgCl/KCl agar/polychloroprene electrode was fabricated based on this paper and proved, as the previous electrode, to be stable and insensitive to pH and  $\text{Cl}^-$ , and with the added polychloroprene layer the problem of electrode degradation in solution was eliminated. This Ag/AgCl/KCl agar/polychloroprene electrode was extremely difficult to fabricate, thus an improvement in design was developed. The reference electrode fabricated with the shrink tubing body was a reproducible design and was stable, with a potential nearly identical to that of a commercial saturated Ag/AgCl electrode, as shown in Figure 3-1. The electrode was also insensitive to pH and  $[\text{Cl}^-]$ , as shown by the black line in the calibration curves in Figure 3-2.

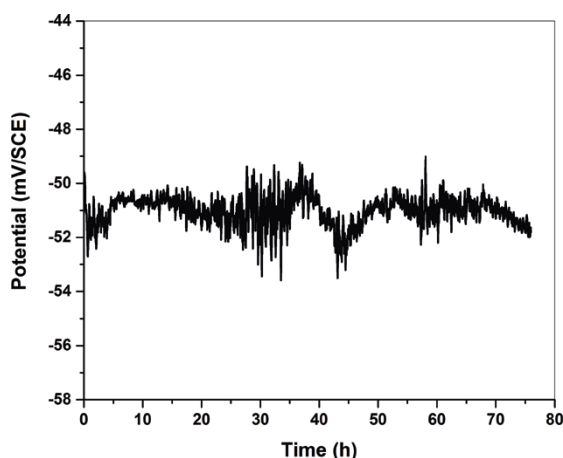


**Figure 3-1.**  $E_{oc}$  of the re-designed Ag/AgCl/KCl agar/polychloroprene electrode in 0.5 M NaCl.

### 3.1.2 pH electrode calibration

Electrochemically oxidized Ir forms a film of various anhydrous and hydrated species including IrO<sub>2</sub>, IrO<sub>2</sub>·4H<sub>2</sub>O, and Ir(OH)<sub>4</sub>·2H<sub>2</sub>O. The anhydrous form, IrO<sub>2</sub>, responds to changes in pH with a slope close to 59 mV (= 2.303 RT/nF) per pH unit via the following equilibria (Hitchman and Ramanathan 1988),



or



The Ir/IrO<sub>2</sub> electrode was calibrated against buffers of pH 4, 7 and 10, as shown in Figure 3-2a. The response of the iridium/iridium oxide pH electrode varies from Nernstian to super-Nernstian, based on the specific iridium species present, thus any changes in the ratio of oxides and hydrates present will have an effect the pH dependence. Our substitution of the air stabilization for the pre-measurement scanning step used by Hitchman and Ramanathan could account for the difference in pH dependence between their electrode (75–81 mV/pH unit) and ours (53 mV/pH).

### 3.1.3 Ion specific electrode calibration

The ion specific electrode chosen to detect changes in chloride concentration is the Ag/AgCl electrode. The electrode responds to changes in [Cl<sup>-</sup>] by sensing a shift in the position of the equilibrium:



The electrode was calibrated against NaCl solutions ranging in concentration from 0.01 M to 1.0 M as shown in Figure 3-2b.

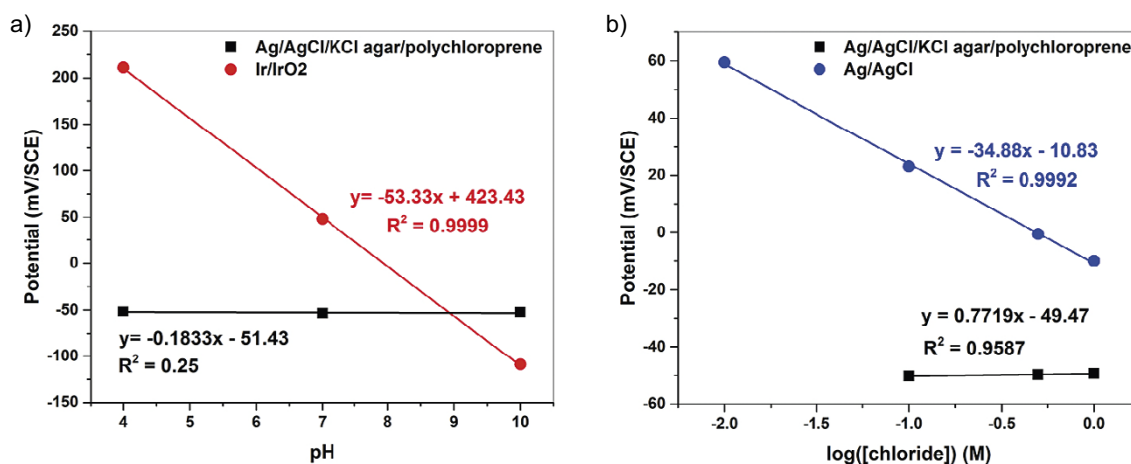


**Figure 3-2.** Calibration curves obtained for: (a) Ir/IrO<sub>2</sub> pH-sensitive electrode and (b) Ag/AgCl Cl<sup>-</sup> ion specific electrode. Black lines show insensitivity of Ag/AgCl/KCl agar/polychloroprene reference electrode in changing pH and Cl<sup>-</sup> environments.

### 3.2 Initial bentonite porewater measurements

$E_{oc}$  (open circuit potential) and  $E_{corr}$  (corrosion potential) measurements were collected for a total of 8 electrodes; 4 surface, and 4 embedded. Each set of electrodes (surface and embedded) included a reference, pH,  $Cl^-$ -specific and Cu electrode, a schematic of the holder and electrode set-up is shown in Figure 3-3. All potentials were measured against a macro saturated calomel electrode (SCE) located in the surrounding bulk aqueous phase, then corrected for the membrane potential of the bentonite layer. Potential measurements,  $E_{measured}$ , made between the SCE and surface/embedded reference electrodes allowed for membrane potential,  $E_{membrane}$ , and ionic strength corrections since,

$$E_{measured} = E_{OC} + E_{membrane} \quad (3-4)$$

where  $E_{oc}$  is the potential difference measured between the SCE and reference electrodes in bulk solution prior to assembly. Since the correction was made for each data point collected, this accounted for changes in ionic strength at the bentonite/electrode interface as clay saturation increased over time. This correction assumed that the  $E_{membrane}$  at the surface/embedded reference electrode was the same as that at the location of each surface/embedded sensor electrode, respectively. It is likely that a similar environment, and therefore a similar  $E_{membrane}$ , was achieved at each electrode, provided that the clay was reasonably homogeneous, as the embedded electrodes were all compacted into the clay at similar depths and the design of the holder allowed for even solution uptake across the bentonite clay disk surface.

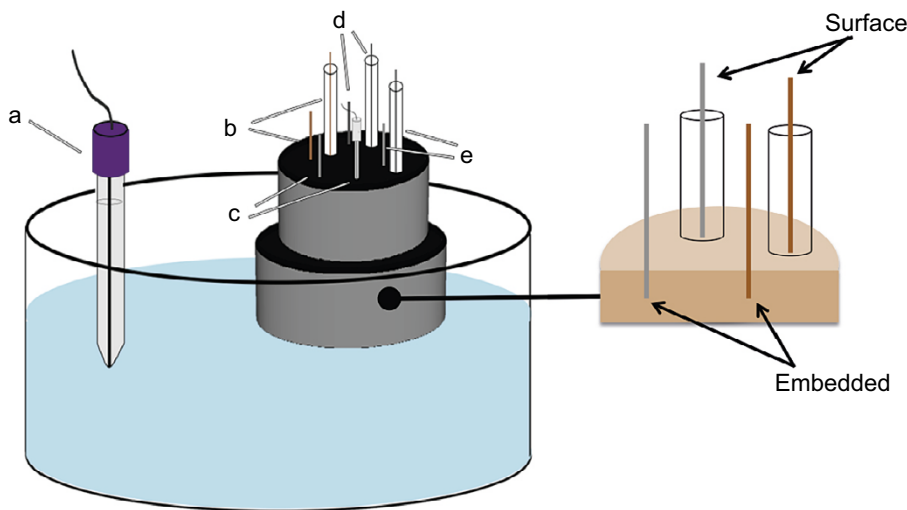
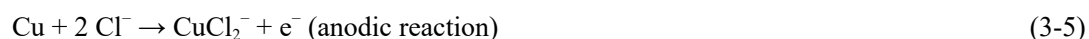


**Figure 3-3.** Schematic of the bentonite disk and holder assembled with the surface and embedded electrodes: (a) SCE reference electrode; (b) Cu electrodes; (c) reference electrodes; (d) chloride sensitive electrodes; (e) pH sensitive electrodes. Cross-section of bentonite disk shows example of surface and embedded electrode placement with just the ends of the surface electrodes in contact with the bentonite.

Once  $E_{\text{membrane}}$  corrections were applied to sensor measurements, reliable values could be obtained regarding the chemistry at the surface of the clay disk as well as inside the clay. A sample of the data collected is shown in Figure 3-4, and steady-state measurements of pH,  $[\text{Cl}^-]$  and  $E_{\text{corr}}$  of the Cu electrode are summarized in Table 3-1. Experiments were run until a steady state was attained. The time required to achieve steady-state was dependent on bentonite thickness; a disk with a thickness of 8 mm was used to allow for proper embedding of the electrodes, and experiments typically reached steady state at around 250 hours. Bradbury and Baeyens (2009) found that MX-80 bentonite exhibited buffering characteristics due to amphoteric hydroxyl groups on the edges of the montmorillonite, and showed a buffering capacity between pH 3 and 11, with the pH staying close to 8. Outside of this range the montmorillonite became unstable and dissolved. The authors found that the overall pH ranged between 6.8 and 8.5 upon exposure to acidic, neutral and basic solutions; initial experiments summarized in Table 3-1 yielded pH values that fell in this range. The  $[\text{Cl}^-]$  measured at the embedded electrodes are lower than those measured at the surface. At 0.5 M, the  $[\text{Cl}^-]$  at the clay disk surface was higher than that in the bulk solution (Figure 3-4c). This is an interesting result that was observed in repeat experiments; however, the reason for it remains unclear at this point. One could imagine a possibility that halite crystals naturally present in the bentonite, when dissolved in the very small volume of water present in the clay exposed to aqueous solution could generate such a high  $[\text{Cl}^-]$ , but if this were the cause, then the same  $[\text{Cl}^-]$  should have been observed in experiments employing 0.1 M NaCl bulk solutions. Another possibility is that there is a problem with the membrane potential correction in this solution, leading to an erroneous high  $[\text{Cl}^-]$ . Further investigation is necessary. The  $E_{\text{corr}}$  measured at the Cu electrode suggests the formation of  $\text{Cu}_2\text{O}$ , the main Cu oxide predicted in the oxic stage, or formation of a Cu chloride complex,  $\text{CuCl}_2^-$ . However, the  $E_{\text{corr}}$  shifts to a more negative potential upon an increase in  $[\text{Cl}^-]$  (Table 3-1), but shows little dependence on pH. This was expected, as the corrosion of Cu in the presence of chloride under aerated conditions proceeds via potential-dependent reactions (Deslouis et al. 1988).



The formation of  $\text{Cu}_2\text{O}$ , which is dependent on the  $[\text{Cl}^-]$  as well as pH, occurs via a precipitation reaction. As  $\text{CuCl}_2^-$  is produced by electrochemical dissolution of Cu (reaction (3-5)), the equilibrium shifts to the right and  $\text{Cu}_2\text{O}$  is deposited (Kear et al. 2004),



with the stability of the oxide being inversely proportional to the  $[\text{Cl}^-]$ . Chloride ions will affect the stability and properties of the precipitated  $\text{Cu}_2\text{O}$  film by incorporation into the oxide lattice via  $\text{Cl}^-$  substitution for  $\text{O}^{2-}$ , which produces defects (King et al. 2002). Since reaction (3-7) shows no potential dependence, any effect of pH would not be observed in  $E_{\text{corr}}$  measurements. This however has not been proven experimentally.

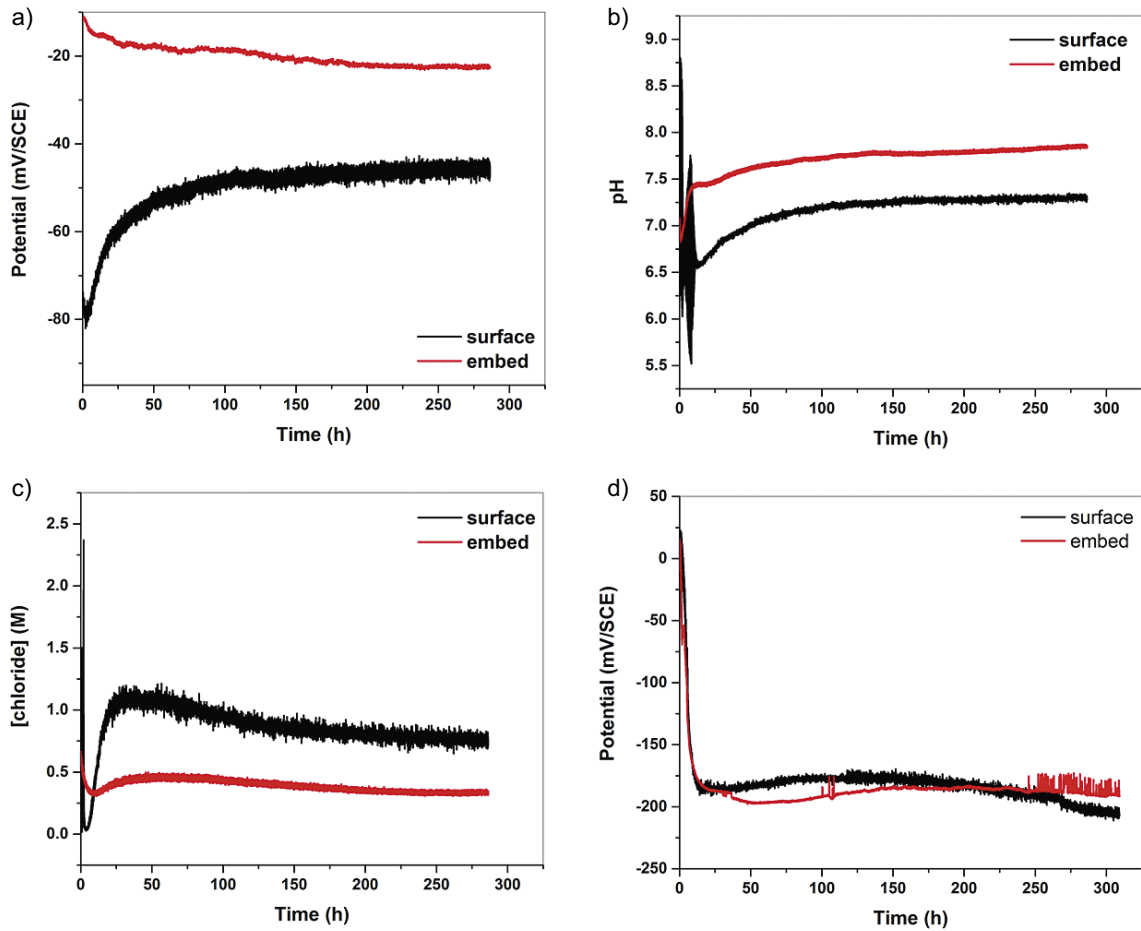


**Figure 3-4.** Experimental data obtained in 0.5 M NaCl solution at the surface and embedded electrodes; (a) reference potentials; (b) pH; (c) [Cl<sup>-</sup>]; (d)  $E_{corr}$  of the Cu electrode.

**Table 3-1. Summary of pH, chloride concentration and steady-state  $E_{corr}$  values obtained from surface and embedded electrodes upon exposure of a bentonite disk to various NaCl solutions.**

Experiment		pH	[Cl <sup>-</sup> ] (M)	$E_{corr}$ (mV/SCE)
(1)	0.1 M NaCl pH = 6.09	S: 6.7	S: 0.091	S: -84
		E: 8.2	E: 0.027	E: -165
(2)	0.1 M NaCl pH = 6.09	S: 8.7	S: 0.03	S: -50
		E: -	E: 0.024	E: -89
(3)	0.5 M NaCl pH = 6.16	S: 7.6	S: 0.64	S: -210
		E: 7.6	E: 0.55	E: -190
(4)	0.5 M NaCl pH = 6.16	S: 7.3	S: 0.76	S: -202
		E: 7.8	E: 0.33	E: -186
(5)	0.5 M NaCl pH = 6.16	S: 7.4	S: -	S: -220
		E: 7.1	E: 0.31	E: -168

### 3.3 Testing the validity of the experimental set-up

#### 3.3.1 Stability of the agar reference electrode

Although the new Ag/AgCl/KCl agar/polychloroprene reference (agar reference) electrode proved to be stable in bulk solutions while pH and chloride concentration were varied, experimental data suggested that the electrode may not necessarily have been stable as a surface reference electrode. Figure 3-5 shows the pH, chloride concentration and the  $E_{\text{corr}}$  of Cu in the bentonite porewater as bulk solution uptake occurred. Substantial drift of the surface chloride concentration, Figure 3-5b, is observed after approximately 150 hours, a time at which a relatively stable reading is expected. Inspection of the surface reference electrode potential, Figure 3-6, shows a potential drift at about the same time (denoted by a dotted line). It is possible that the drift of the surface agar reference electrode, and therefore apparent (but not valid) changes in the membrane potential, ultimately was the cause of the unreasonable chloride concentration obtained after the membrane potential correction.

To test whether this was the case, we explored the consequences of a hypothetical situation in which we postulate that the membrane potential of the agar reference did not change (drift) after the 150-hour mark. Using this constant membrane potential (that determined at the 150-hour mark), the pH, chloride concentration and  $E_{\text{corr}}$  surface measurements were recalculated (shown in Figure 3-7). After this correction was applied, an appreciable difference was observed in the pH and chloride concentration values, Figure 3-7a and b. This suggested that the increase observed at about 150 hours was likely due to the drift of the agar reference surface electrode and not representative of a chemical change in the bentonite clay system. However, little change was observed with respect to the  $E_{\text{corr}}$  of Cu after the new correction was made, Figure 3-7c. The reason for the small shift in the  $E_{\text{corr}}$  of Cu compared to that of the pH and  $[\text{Cl}^-]$  is the former has a linear relationship with the reference electrode, whereas the latter two depend exponentially on potential.

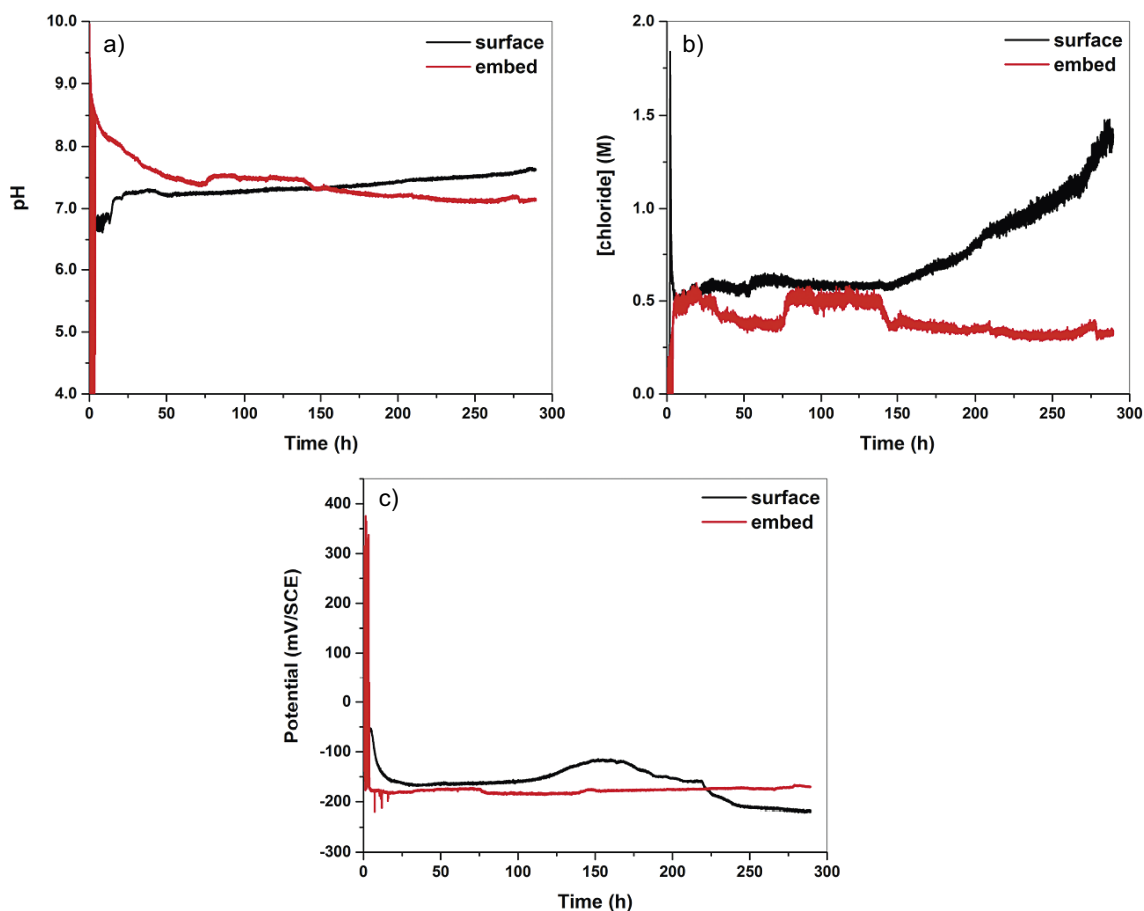


**Figure 3-5.** Experimental data obtained in 0.5 M NaCl solution with the use of both surface and embedded agar reference electrodes; (a) pH; (b)  $[\text{Cl}^-]$ ; (c)  $E_{\text{corr}}$  of the Cu electrode.

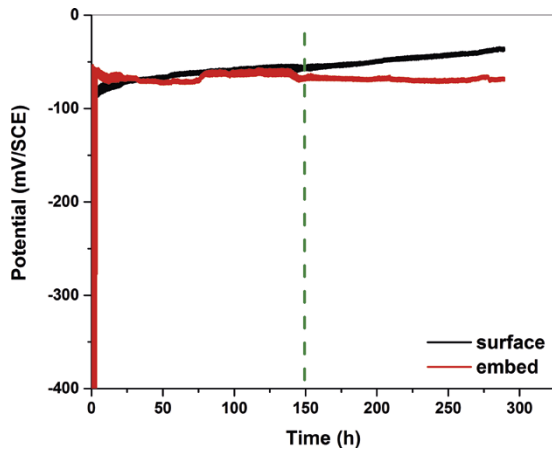


**Figure 3-6.** Agar reference electrode potentials measured at surface and embedded sites in 0.5 M NaCl solution. Dashed line denotes potential drift starting at 150 hours.

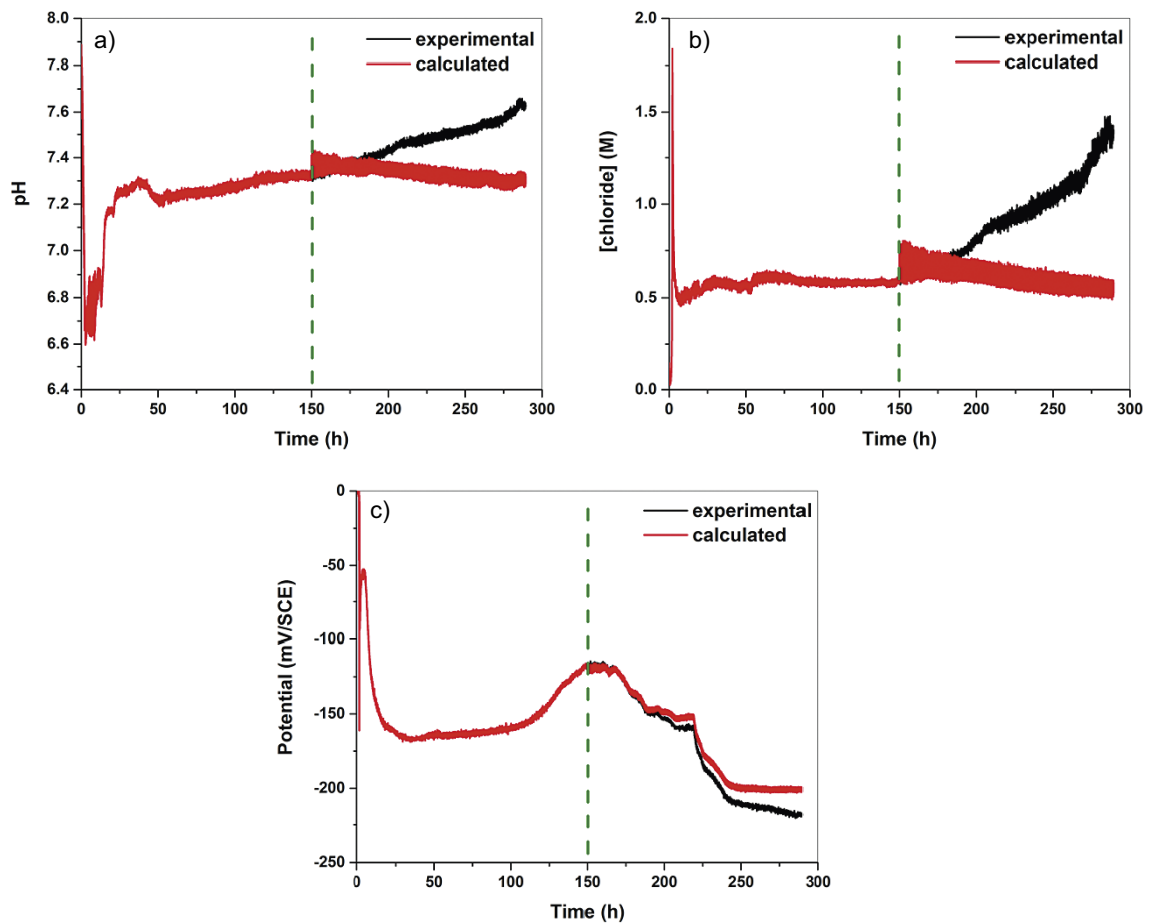


**Figure 3-7.** Overlay of experimental and calculated (corrected) data for the surface electrodes in 0.5 M NaCl. Dashed line indicates where new membrane potential was used to correct data.

### 3.3.2 Measuring membrane potentials across the bentonite clay disk

The apparent instability of the agar reference electrode in the experimental setup is important to address, as its potential is used to calculate membrane potentials as the clay saturates with solution over time. Without a reliable membrane potential value, the subsequent calculations of the pH,  $[Cl^-]$  and  $E_{corr}$  of Cu will not yield reliable data. As described in Section 3.2, the membrane potential correction relies on the assumption that the agar reference electrode is stable and experiences the same environment as each of the electrodes in the same set (i.e., the surface reference electrode experiences the same environment as the pH,  $Cl^-$ -specific and Cu surface electrodes). To legitimize this assumption a bentonite experiment was assembled with agar reference electrodes placed at various locations, both on the surface and inside the clay disk. This experiment addressed two main concerns; (i) whether all the sites experience equivalent conditions and therefore exhibit similar membrane potentials and (ii) the stability of the surface agar reference electrode. In this experiment 6 agar reference electrodes were fabricated; 3 electrodes were placed on the surface and 3 were embedded inside the bentonite disk. The measurement results are shown in Figure 3-8; however, the results from only two surface electrodes are presented as one malfunctioned during the course of the experiment. It is clear from Figure 3-9 that the membrane potentials collected both at the clay surface and at embedded sites are not equal. There were membrane potential differences of 26 mV and 35 mV for the surface and embedded sites, respectively. Such large potential differences are troubling, as these results invalidate the earlier assumption proposed in Section 3.2 and thus call into question the accuracy of the pH,  $[Cl^-]$  and  $E_{corr}$  values collected previously.

During this experiment, however, all electrodes were relatively stable and did not experience a large drift once the clay was saturated, as seen in the previous experiment. We concluded that the surface electrodes experience a drift over time when poor contact is made between the electrode and the clay surface. This could be easily addressed by increasing the weight of the agar reference electrode; perhaps by constructing the electrode body out of glass as instead of PTFE shrink tubing or adding a small weight to help push it down against the clay. Increased electrode weight would ensure sufficient contact with the bentonite surface and help to eliminate drift artifacts.

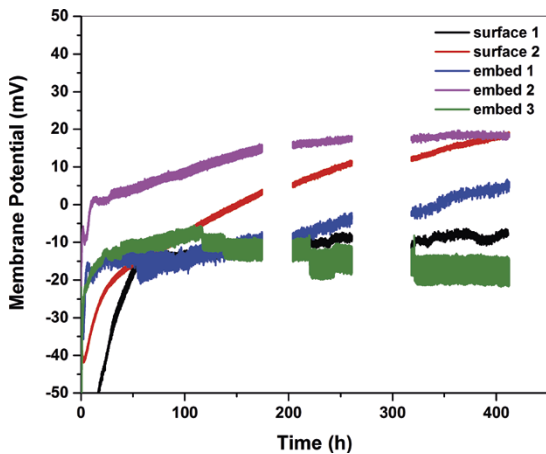


**Figure 3-8.** Membrane potentials obtained for surface and embedded agar reference electrodes in 0.5 M NaCl solution. Breaks in data due to computer failure.

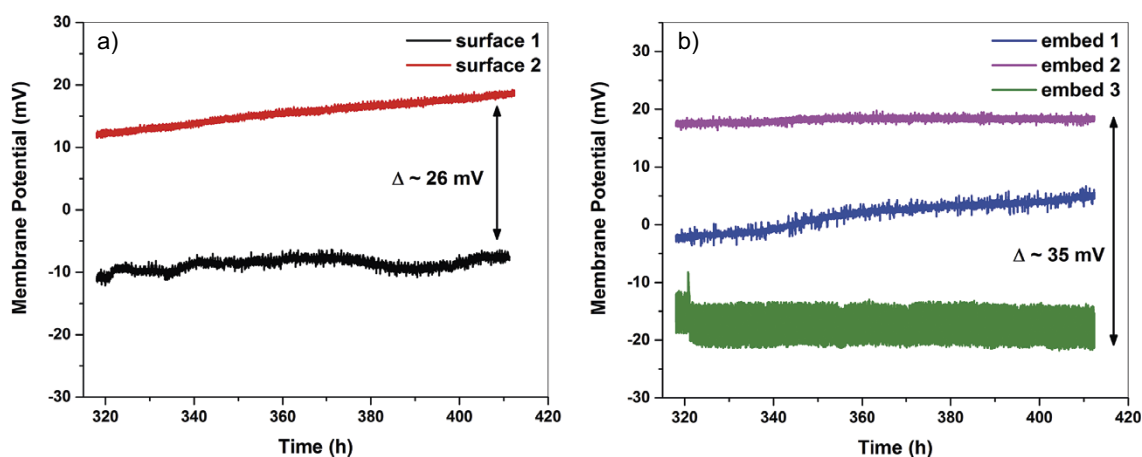


**Figure 3-9.** Steady-state membrane potentials measured at the end of the experiment shown in Figure 3-8 for (a) surface agar reference electrodes; (b) embedded agar reference electrodes. Arrow indicates maximum difference in membrane potential.

The problem regarding the large differences in the membrane potential values collected across the bentonite clay needs to be addressed before further measurements can be made. The variation in the membrane potential could be due to inhomogeneity of the bentonite clay disk and/or changes to the  $E_{oc}$  of the agar reference electrode due to contact with the bentonite. An additional experiment was completed in an attempt to determine if one, or both, of these proposed situations were responsible for the difference in the collected membrane potentials. In this new experiment, the apparent membrane potential at 3 locations on the surface of the clay was monitored with each of 3 different agar reference electrodes (Figure 3-10). The potential difference between the surface reference electrode in contact with bentonite and the SCE in bulk solution at each location was determined with each electrode, and membrane potentials were calculated for each combination of electrode and surface position.

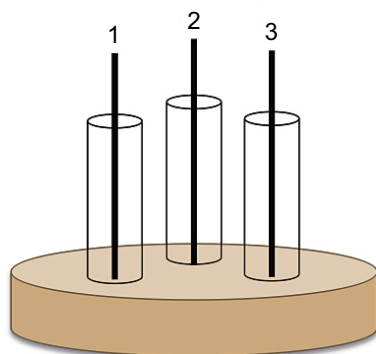


**Figure 3-10.** Set-up of 3 agar reference electrodes placed at 3 different locations across the bentonite disk surface. PTFE holder is omitted from schematic.

The membrane potentials summarized by surface location are shown in Figure 3-11. The variances in membrane potential for each electrode at locations 1, 2 and 3 are 18 mV, 10 mV and 15 mV, respectively. Alternatively, the results summarized by electrode are shown in Figure 3-12. A smaller variance in membrane potential is generally observed, with variances of 13 mV, 6 mV and 3 mV for electrodes 1, 2 and 3, respectively. Assuming electrode 1 had a defect of some sort, overall, electrodes 2 and 3 show very little difference in their membrane potentials, irrespective of their location on the clay. The fact that each electrode has a different, yet consistent, membrane potential across the clay surface suggests that the membrane potential discrepancy is due to changes to the agar reference electrode, not due to inhomogeneities within the bentonite.

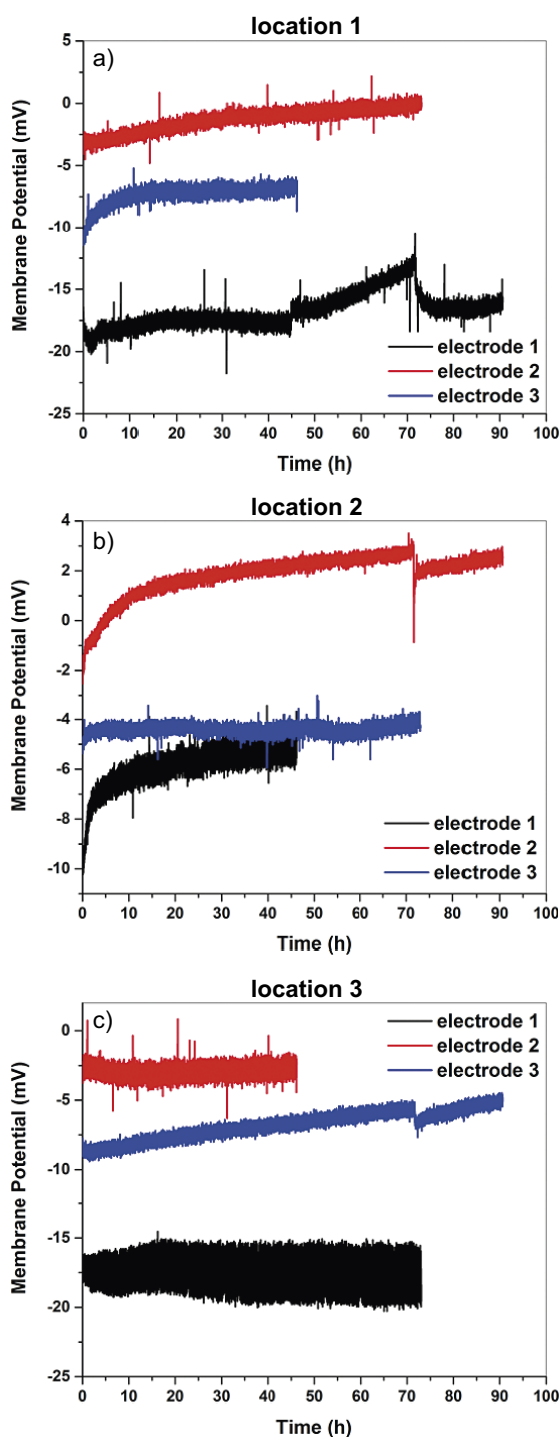


**Figure 3-11.** Membrane potentials measured by 3 agar reference electrodes in 0.5 M NaCl solution at (a) location 1; (b) location 2; (c) location 3 across the bentonite clay surface.

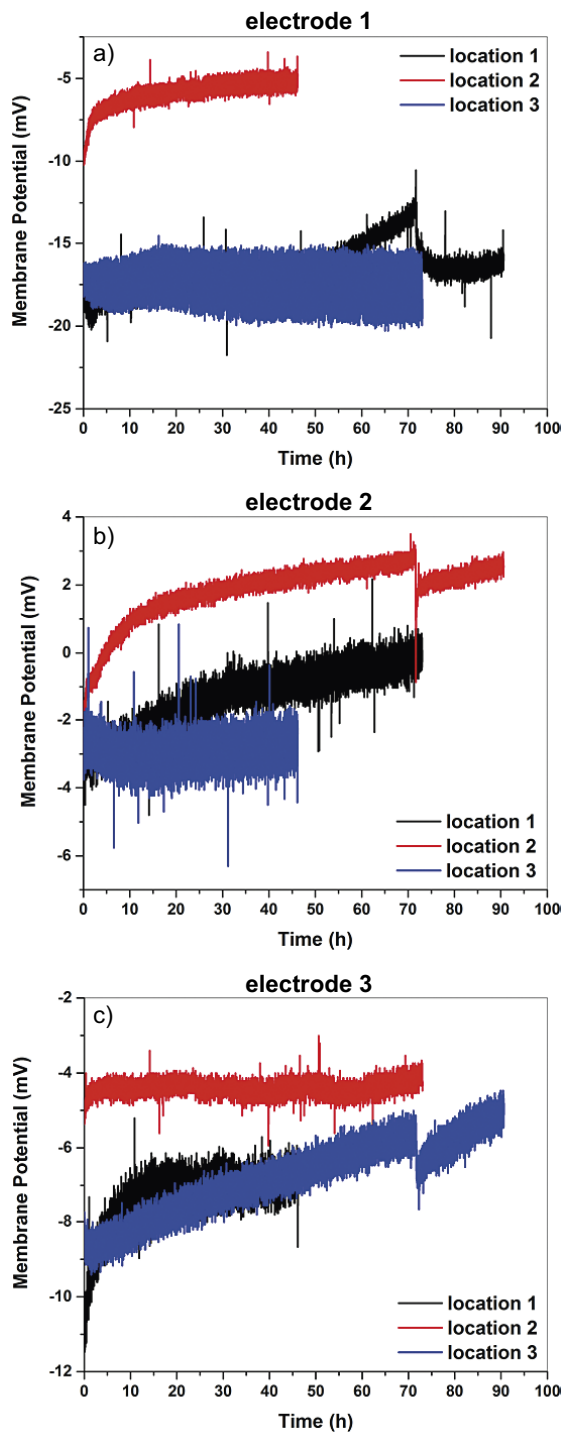


**Figure 3-12.** Membrane potentials measured at 3 locations across the bentonite clay surface in 0.5 M NaCl solution by (a) electrode 1; (b) electrode 2; (c) electrode 3.

To check whether the agar reference electrode experiences a change to its own membrane potential after contact with the bentonite, the  $E_{oc}$  of each of the 3 agar reference electrodes was measured once the aforementioned experiment was complete. The electrode/bentonite membrane potentials were then recalculated based on the new  $E_{oc}$  measurements obtained post interaction between electrode and clay. The recalculated values plotted by location are shown in Figure 3-13 (the recalculated values plotted by electrode are not shown here, as they simply show a small change in magnitude, but no change with respect to each other). With these recalculated measurements the variances in membrane potential over the 3 electrodes at locations 1, 2 and 3 were 6 mV, 13 mV and 3 mV, respectively. With this correction, we see that 2/3 sets of membrane potentials collected, whether examined by bentonite

location or by agar reference electrode, show a reasonable variance in membrane potential of 6 mV or less. This suggests that if the agar reference electrode is modified upon interaction with the bentonite clay before the experiment is performed, the calculated membrane potentials at the sensor/clay interface will be relatively constant across the bentonite disk. Ultimately, this proves that the assumption made in Section 3.2 is in fact valid, and the current set-up can be used to complete future experiments.

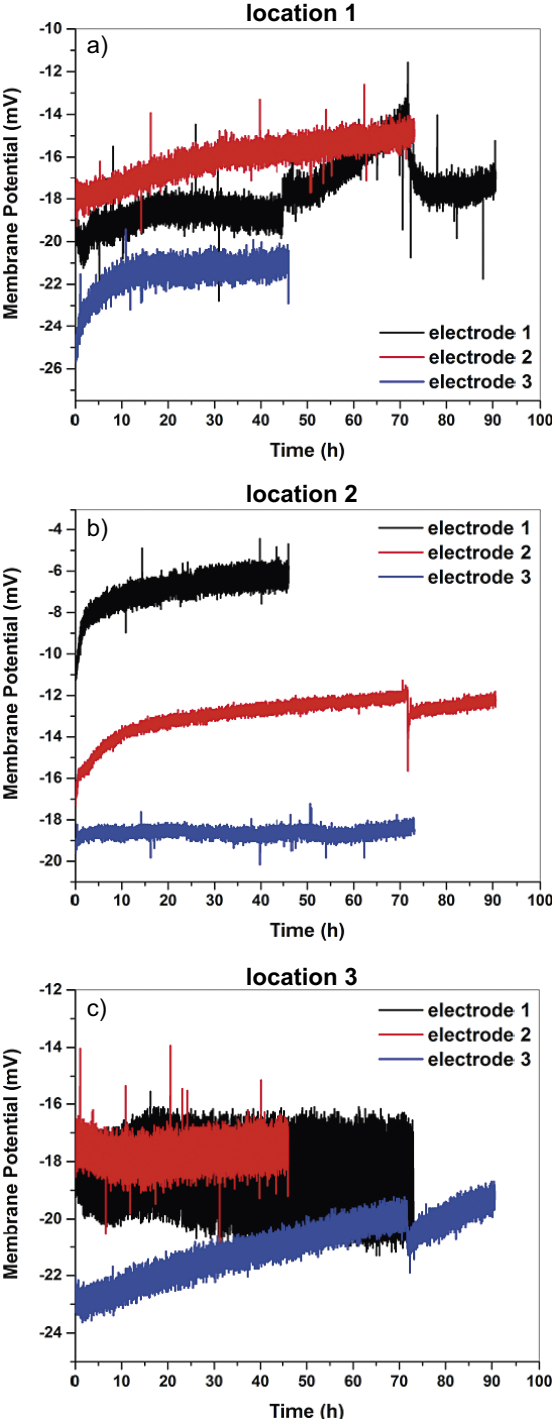


**Figure 3-13.** Recalculated membrane potentials measured by 3 agar reference electrodes in 0.5 M NaCl solution at (a) location 1; (b) location 2; (c) location 3 across the bentonite clay surface.

In principle, one could use these data to test different hypotheses regarding the pore water chemistry. For instance, using formulae provided by Idiart and Peřkala (2016) and the measured membrane potentials, one could calculate the ion equilibrium coefficient (or Donnan factor) of the system, which, assuming that the solution composition was governed by a Donnan equilibrium, could then be used to predict the activities of ions at the clay-covered electrode surfaces. These predictions could then be compared with the concentrations measured at the sensor electrodes. Although better data would increase the confidence in such an analysis, we demonstrate the process using the recalculated membrane potentials of Figure 3-13 and choosing a typical value in the range of about  $-20$  mV for this exercise. From Idiart and Peřkala (2016), we have,

$$\Xi = \exp\left(\frac{F\varphi}{RT}\right) \quad (3-8)$$

where  $\Xi$  is the ion equilibrium coefficient,  $F$  Faraday's constant ( $96485$  C/equivalent),  $\varphi$  the measured membrane potential (e.g.,  $-20$  mV),  $R$  the universal gas constant ( $8.314$  C $\cdot$ V $\cdot$ K $^{-1}$  $\cdot$ mol $^{-1}$ ) and  $T$  the absolute temperature (e.g.,  $298$  K). Using these values yields  $\Xi = 0.45$ , which can then be used to calculate the ratio of ion activities on either side of the clay membrane by,

$$\frac{a_i^{int}}{a_i^{ext}} = \Xi^{-Z_i} \quad (3-9)$$

where  $a_i$  indicates the activity of ion  $i$  in either the solution in the bentonite interior (int) or the external bulk solution (ext) and  $Z_i$  is the charge on ion  $i$  ( $= -1$  for  $\text{Cl}^-$  ions). For an ion equilibrium coefficient of  $0.45$  and the bulk NaCl concentration of  $0.5$  M ( $a_{\text{Cl}^-}^{ext} = \gamma_{\text{Cl}^-} [\text{Cl}^-] = \left(0.684 \frac{\text{L}}{\text{mol}}\right) \left(0.5 \frac{\text{mol}}{\text{L}}\right) = 0.342$ , where  $\gamma_{\text{Cl}^-}$  is the activity coefficient of  $\text{Cl}^-$ ), we can calculate (Equation 3-9) that  $a_i^{int} = 0.154$  and  $[\text{Cl}^-]$  in the interior of the bentonite should be  $\sim 0.21$  M, based on activity coefficients from Partanen and Partanen (2020). This differs substantially from the measured chloride concentration values in Figure 3-7, suggesting that the composition of the free porewater and surface water under the clay membrane is not controlled by a Donnan equilibrium under these conditions but again, better data would increase the confidence in this analysis.



## 4 Key results and future work

- A new Ag/AgCl/KCl agar/polychloroprene reference electrode was fabricated. This electrode provided good stability and was insensitive to pH and chloride concentration. It was successfully embedded into the bentonite and used to measure the membrane potential across the bentonite clay disk, a value needed for determining the pH,  $[Cl^-]$ , and  $E_{corr}$  of Cu on both the surface of the bentonite clay disk and its interior using sensor electrodes.
- An experimental set-up has been successfully developed for monitoring the pH,  $[Cl^-]$ , and  $E_{corr}$  of Cu on both the surface of the bentonite clay disk and its interior.
- The instability of the agar electrode, which ultimately affects the reliability of the final pH,  $[Cl^-]$ , and  $E_{corr}$  values, was determined to result from poor contact with the bentonite clay. We propose that this surface reference electrode be fabricated out of a heavier material to minimize or eliminate this problem.
- The membrane potentials across the clay surface were measured with multiple agar reference electrodes. We found that upon interaction with the bentonite the potential of the agar electrode itself was modified, possibly by changing the junction potential of the polychloroprene membrane of the agar electrode or by introducing a phase boundary potential involving the charged particles of the clay. Once changes in the electrode are taken into consideration, the maximum variance in membrane potential across the surface is about 6 mV. This small potential difference validates the earlier assumption that the various sensors experience roughly the same environment at each location across the bentonite disk surface. This validation supports further use of the current set-up for future experiments.
- While no definite conclusions can be made at this time regarding the types of water present in the clay, results obtained thus far coincide with previous data regarding the chemical composition of the bentonite porewater.
- Future goals include:
  - Determining the effect that the bentonite clay has on the agar reference electrode potential and ultimately its affect on membrane potential.
  - Determining steady-state pH and chloride concentrations for bentonite exposed to a wide range of solutions, as well as determination of the rate of chloride ion migration through the clay in anoxic environments or upon exposure to sulphide.
  - Studying accumulation and hyperfiltration effects by placing electrodes at the bentonite/filter interface.
  - Maintaining better control of the bentonite dry density by using a more robust holder.
  - Maintaining bentonite conditions that are as homogeneous and well-defined as possible by starting experiments with fully water saturated bentonite layers.
  - Ensuring that ionic activities within the bentonite are fully equilibrated by the end of each experiment, to improve the reliability of our data.



## References

SKB's (Svensk Kärnbränslehantering AB) publications can be found at [www.skb.com/publications](http://www.skb.com/publications).

- Arcos D, Grandia F, Domènech C, 2006.** Geochemical evolution of the near field of a KBS-3 repository. SKB TR-06-16, Svensk Kärnbränslehantering AB.
- Auqué L F, Gimeno M J, Gómez J B, Puigdomenech I, Smellie J, Tullborg E-L, 2006.** Groundwater chemistry around a repository for spent nuclear fuel over a glacial cycle. Evaluation for SR-Can. SKB TR-06-31, Svensk Kärnbränslehantering AB.
- Berglund S, Lindborg T (eds), 2017.** Monitoring Forsmark – evaluation and recommendations for programme update. SKB TR-15-01, Svensk Kärnbränslehantering AB.
- Bradbury M H, Baeyens B, 2003.** Porewater chemistry in compacted re-saturated MX-80 bentonite. *Journal of Contaminant Hydrology* 61, 329–338.
- Bradbury M H, Baeyens B, 2009.** Experimental and modelling studies on the pH buffering of MX-80 bentonite porewater. *Applied Geochemistry* 24, 419–425.
- Bruno J, Arcos D, Duro L, 1999.** Processes and features affecting the near field hydrochemistry. Groundwater-bentonite interaction. SKB TR-99-29, Svensk Kärnbränslehantering AB.
- Cuevas J, Villar M V, Fernández A M, Gómez P, Martín P L, 1997.** Pore waters extracted from compacted bentonite subjected to simultaneous heating and hydration. *Applied Geochemistry* 12, 473–481.
- Deslouis C, Tribollet B, Mengoli G, Musiani M M, 1988.** Electrochemical behaviour of copper in neutral aerated chloride solution. I. Steady-state investigation. *Journal of Applied Electrochemistry* 18, 374–383.
- Hitchman M L, Ramanathan S, 1988.** Evaluation of iridium oxide electrodes formed by potential cycling as pH probes. *Analyst* 113, 35–39.
- Huang I-Y, Huang R-S, Lo L-H, 2003.** Improvement of integrated Ag/AgCl thin-film electrodes by KCl-gel coating for ISFET applications. *Sensors and Actuators B: Chemical* 94, 53–64.
- Idiart A, Pekala M, 2016.** Models for diffusion in compacted bentonite. SKB TR-15-06, Svensk Kärnbränslehantering AB.
- Kear G, Barker B D, Walsh F C, 2004.** Electrochemical corrosion of unalloyed copper in chloride media – a critical review. *Corrosion Science* 46, 109–135.
- Kim T Y, Hong S A, Yang S, 2015.** A solid-state thin-film Ag/AgCl reference electrode coated with graphene oxide and its use in a pH sensor. *Sensors* 15, 6469–6482.
- King F, 2002.** Corrosion of copper in alkaline chloride environments. SKB TR-02-25, Svensk Kärnbränslehantering AB.
- King F, 2009.** Microbiologically influenced corrosion of nuclear waste containers. *Corrosion* 65, 233–251.
- King F, 2013.** Container materials for the storage and disposal of nuclear waste. *Corrosion* 69, 986–1011.
- King F, Ahonen L, Taxén C, Vuorinen U, Werme L, 2002.** Copper corrosion under expected conditions in a deep geologic repository. Posiva 2002-01, Posiva Oy, Finland.
- King F, Lilja C, Pedersen K, Pitkänen P, Vähänen M, 2010.** An update of the state-of-the-art report on the corrosion of copper under expected conditions in a deep geologic repository. SKB TR-10-67, Svensk Kärnbränslehantering AB.
- King F, Lilja C, Vähänen M, 2013.** Progress in the understanding of the long-term corrosion behaviour of copper canisters. *Journal of Nuclear Materials* 438, 228–237.

- Kinlen P J, Heider J E, Hubbard D E, 1994.** A solid-state pH sensor based on a Nafion-coated iridium oxide indicator electrode and a polymer-based silver chloride reference electrode. *Sensors and Actuators B: Chemical* 22, 13–25.
- Kosec T, Kranjc A, Rosborg B, Legat A, 2015.** Post examination of copper ER sensors exposed to bentonite. *Journal of Nuclear Materials* 459, 306–312.
- Kwon N-H, Lee K-S, Won M-S, Shim Y-B, 2007.** An all-solid-state reference electrode based on the layer-by-layer polymer coating. *Analyst* 132, 906–912.
- Liao W-Y, Chou T-C, 2006.** Fabrication of a planar-form screen-printed solid electrolyte modified Ag/AgCl reference electrode for application in a potentiometric biosensor. *Analytical Chemistry* 78, 4219–4223.
- Nolan M A, Tan S H, Kounaves S P, 1997.** Fabrication and characterization of a solid state reference electrode for electroanalysis of natural waters with ultramicroelectrodes. *Analytical Chemistry* 69, 1244–1247.
- Partanen L J, Partanen J I, 2020.** Traceable values for activity and osmotic coefficients in aqueous sodium chloride solutions at temperatures from 273.15 to 373.15 K up to the saturated solutions. *Journal of Chemical & Engineering Data* 65, 5226–5239.
- Rosborg B, Pan J, 2008.** An electrochemical impedance spectroscopy study of copper in a bentonite/saline groundwater environment. *Electrochimica Acta* 53, 7556–7564.
- Rosborg B, Kosec T, Kranjc A, Pan J, Legat A, 2011.** Electrochemical impedance spectroscopy of pure copper exposed in bentonite under oxic conditions. *Electrochimica Acta* 56, 7862–7870.

SKB is responsible for managing spent nuclear fuel and radioactive waste produced by the Swedish nuclear power plants such that man and the environment are protected in the near and distant future.

**skb.se**